

A search for b(c) quark pdf uncertainties at TeV scale ep collider

H. Aksakal^{1,*} and S. O. Kara^{2,†}

¹*Physics Department, Art and Science Faculty Nigde University, Nigde, Turkey*

²*Bor Vocational School, Nigde University, Nigde, Turkey*

Abstract

We discuss $c\bar{c}$ and $b\bar{b}$ pair productions at ep collider for studying extremely small $x(g)$ region. It has been shown that Large Hadron electron Collider (LHeC) has a reach of about $x(g) > 10^{-6}$. The aim of this work is to show that the PDF uncertainties in the heavy flavour production. Maximum difference of cross section between PDFs 60% has been found in the process of $ep \rightarrow eq\bar{q}X$.

arXiv:1306.4764v1 [hep-ph] 20 Jun 2013

* aksakal@cern.ch

† seytokankara@gmail.com

1. INTRODUCTION

The Large Hadron Collider (LHC) will provide unique physics opportunities for SM and BSM physics. In hadron colliders, one of the sources of the systematic errors on the measured quantities is the uncertainty in the parton distribution functions (PDFs). The current proton PDF knowledge mostly originates from the deep inelastic scattering (DIS) measurements at the first ep collider, HERA. It has probed small $x(g)$ region and had a reach of about $x(g) > 10^{-4}$. Probing even smaller $x(g)$ region [1] could be realized with the Large Hadron Electron Collider (LHeC) project [2]. In LHeC, electron beams of 60 and 140 GeV energy accelerated either by a linac (linac-ring version) or by the ring installed in LHC tunnel (ring-ring version) are collided with 7 TeV LHC protons (or ions).

The photon-gluon fusion in LHeC is to produce heavy flavour quark pairs as it can be seen in Fig.1. In this vertex the gluon flavour PDF uncertainty has to be considered[2]. The gluon PDF is responsible to determine small $x(g)$ region for low momentum fraction. In the conventional QCD framework, the PDFs for charm (c) and bottom (b) quarks are determined by fitting to the hadronic data [3]. In this study the maximum values of differential cross section and corresponding $x(g)$ values have been investigated for several different PDFs in CompHEP [4] software package. Obtained results clearly show the difference between PDFs. The investigation of small $x(g)$ region using the processes $ep \rightarrow ebb\bar{X}$ and $ep \rightarrow ec\bar{X}$ is presented in section 2. In section 3 the accelerator properties of LHeC have been summarized. Finally, the generator level results of PDF distributions with $b\bar{b}$ and $c\bar{c}$ pair production obtained using CompHEP are analyzed in section 4.

2. THE PHYSICS CASE

In the ep option of the LHeC one can consider two cases: firstly e-beam energy with 60 GeV (LHeC Type-1) and second 140 GeV (LHeC Type-2). On the other hand, in another version of the ep collider, the beam energies can be extended to 250 GeV (and/or 500 GeV). The processes $ep \rightarrow ebb\bar{X}$ and $ep \rightarrow ec\bar{X}$ have been used in the PDF uncertainty studies. The subprocesses $eg \rightarrow ebb\bar{b}$ and $eg \rightarrow ec\bar{c}$ have been used to measure of the $x(g)$ where the gluon (g) is from the LHC protons, electrons are from an electron linac. The b quark final states are easier to identify due to b -tagging possibility using currently available technologies:

LHeC and ep collider	$b\bar{b}$ (pb)	$c\bar{c}$ (pb)
LHeC Type-1($E_e = 60\text{GeV}$)	4.19×10^3	2.36×10^5
LHeC Type-2($E_e = 140\text{GeV}$)	6.95×10^3	3.67×10^5
ep collider-1($E_e = 250\text{GeV}$)	9.65×10^3	4.91×10^5
ep collider-2($E_e = 500\text{GeV}$)	1.4×10^4	6.89×10^5

Table I. Heavy quark pair production cross sections for LHeC and ep collider

LHeC and ep collider	$b\bar{b}$		$c\bar{c}$	
	$d\sigma/dx$	x	$d\sigma/dx$	x
LHeC Type-1	$0.49nb$	2.15×10^{-4}	$0.13\mu b$	3.53×10^{-5}
LHeC Type-2	$1.77nb$	9.17×10^{-5}	$0.45\mu b$	1.7×10^{-5}
ep collider-1	$4.19nb$	4.88×10^{-5}	$1.06\mu b$	9.95×10^{-6}
ep collider-2	$10.62nb$	2.75×10^{-5}	$2.6\mu b$	5.15×10^{-6}

Table II. Maximum values of $d\sigma/dx(g)$ and corresponding $x(g)$ values for $b\bar{b}$ and $c\bar{c}$ final states at LHeC and ep collider.

for example, ATLAS silicon detectors have 70% b-tagging efficiency[5].

In Table 1 we introduce the cross sections of heavy quark pair production for LHeC and ep colliders. CTEQ6L1[6, 7] PDF distribution in CompHEP simulation program has been chosen for all calculations in Table 1.

In Table 2, maximum values of differential cross sections and corresponding $x(g)$ values are given for different PDF distributions at LHeC and ep collider. For example the differential cross sections for LHeC Type-1 and LHeC Type-2 achieve maximum values at CTEQ5L, while maximum values for ep collider-1 and ep collider-2 are CTEQ4L and CTEQ5L for $b\bar{b}$, CTEQ6L1 for $c\bar{c}$, respectively.

3. THE ACCELERATOR PROPERTIES

The LHeC can be obtained by using a linac to accelerate $e(e^+$ or $\gamma)$ -beam to 60-140 GeV and colliding with 7 TeV LHC proton beam most realistically from the upgraded LHC. Such a collider has been proposed previously under the name of ‘‘QCD Explorer’’ project

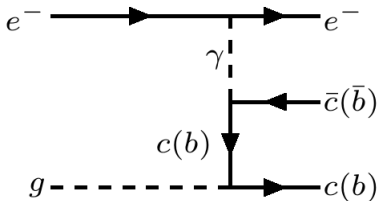


Figure 1. The tree level Feynman diagram for heavy quark pair production

[10, 11]. The linac would be based on superconducting RF technology[2, 12]. The Table III contains the Linac and LHC parameters. To provide the e -beam, so far two accelerator options have been considered. A “ring” option that can be achieved by the installation of an additional e^- (or e^+) ring inside the LHC tunnel[13]. This option has the benefit of having the circulating beams similar to well known LEP operations however the maximum energy that could be provided by the ee^+ beams is rather limited. There are two version of linac option under consideration: multipass energy recovery linac (ERL) and the second a pulsed linac. First one has 10^{33} luminosity can not reach more than 60 GeV beam energy because of rigorous synchrotron radiation. In the second option, the e-beam energy can be obtained by the utilization of linac[2]. The second option have two possibilities which are: an ILC like SC linac and a NC linac. Efficient positron production for e^+p collision at LHeC is explained in Ref.[14]. $\gamma - p$ collision at LHeC is also possible where γ comes from Compton backscattering of laser photons off e -beam and it is an advantage for Linac-ring option but not possible for the ring-ring one[15, 16]. An additional benefit of a linac is the possibility of high electron (thus photon) polarization. The luminosity of the collider has been calculated by CAIN code [17] which was originally written for $e^-(e^+ \text{ or } \gamma) - e^-(e^+ \text{ or } \gamma)$ collision and can be easily adopted to ep collision. In the case of LHC upgraded option of Large Pwinski Angle (LPA) [12] is used then number of proton per bunch can be increased by 2.5 times thus the luminosity is also increased by a factor of 2.5.

4. PHYSICS SEARCH POTENTIAL AND PDF UNCERTAINTY

The precise measurement of PDFs play crucial role in the framework of QCD studies. The different differential cross sections obtained from different PDFs originate in PDF uncertainties. Used PDFs can be divided in three groups which are leading order-LO (cteq5l,

parameter	Linac (ERL /pulsed(SC))	LHC
RF Frequency $F_{RF}(GHz)$	0.721/1.3	0.4
Beam energy $E_b (GeV)$	60/140 – 250 – 500	7000
Bunch length $\sigma_z (mm)$	0.3	75.5
Bunch size at IP $\sigma_x/\sigma_y (\mu m)$	7	7
Tr. nor. emittance $\gamma\epsilon_x/\gamma\epsilon_y (\mu m)$	50	3.75
Bunch spacing (ns)	25(or50)/25(or50)	25 (or50)
Rep. Freq. (Hz)	40(or 20) $10^6/10$ (or 5)	NA
# of bunch	$CW/1 10^5$	2808 (or1404)
Bunch length (mm)	0.3	75.5
Bunch population	1(or2) $10^9 /210^9$	1.710^{11}
Average beam current $I (mA)$	6.4/3.2	> 430
$\sqrt{s} TeV$	1.3 1.98 2.64	3.74
Luminosity $10^{32}(cm^{-2}s^{-1})$	9.7 0.68 0.78	0.87

Table III. Linac and LHC Parameters

cteq4l, cteq6l), next-to-leading order-NLO (cteq5m1, cteq6d), and \overline{MS} (cteq4m, cteq6m, cteq6l1). Perturbative correction in DIS (pQCD) includes LO and NLO contribution. \overline{MS} scheme distributions defined by matrix elements are not simple one loop in perturbation theory and for most application \overline{MS} parton distribution is mostly used [18–20]. As seen from Fig.2, the difference is quite evident for large values of \sqrt{s} , whereas it is closely for the center of mass energy less than 1 TeV. Furthermore this figure shows two groups of curves for the larger \sqrt{s} values: the differential cross sections of first group are around at 25 nb and second at 15 nb .

In Fig. 3 differential cross section versus the $x(g)$ reach at LHeC Type-1 is plotted for different PDFs. It is seen that the $d\sigma/dx(g)$ of $c\bar{c}$ pair production is larger than of $b\bar{b}$ pair production. In both final states, CTEQ6L1, CTEQ5L and CTEQ4L adopt a similar manner for large values of $d\sigma/dx(g)$ and the others without CTEQ6L for small values. $d\sigma/dx(g)$ of CTEQ6L achieves maximum value 0.4 nb for $b\bar{b}$ and 0.1 μb for $c\bar{c}$ pair productions.

Similar distributions for $b\bar{b}$ and $c\bar{c}$ pair productions at LHeC Type-2 are shown in Fig. 4. For example, differential cross section of $b\bar{b}$ pair production for CTEQ5L achieves maximum

value 1.77 nb at $x(g) = 9.17 \times 10^{-5}$ whereas that of $c\bar{c}$ pair production for CTEQ5L is $0.45 \mu\text{b}$ at $x(g) = 1.7 \times 10^{-5}$.

In order to show the distributions of PDFs for ep collider-1 we present the Fig. 5, where the shift in the $x(g)$ values of some PDF peaks from the others is clearly seen for $c\bar{c}$ final state. The same shift for $c\bar{c}$ pair production at ep collider-2 is more explicitly seen in Fig. 6. This shift comes from gluon uncertainties which is most uncertain of PDFs and it increases with \sqrt{s} , can be used to choose more appropriate PDF when the experimental data became available.

5. CONCLUSIONS

By investigating the processes $ep \rightarrow e\bar{b}bX$ and $ep \rightarrow ec\bar{c}X$, we have shown that PDFs for LHeC and an ep collider adopt different manner. Obtained peak difference of differential cross sections in between these PDFs is about 60% and it is arise from LO, NLO and \overline{MS} contribution. The difference can be reduced by taken into account unimplemented corrections because total cross section of DIS is not simple finite function of α_s , those unimplemented corrections will be searched as a next publication. As a result of calculations done, we could say that the differential cross sections obtained from different PDFs are closely for the center of mass energy less than 1 TeV, whereas they are quite evidently for large values of \sqrt{s} . The differential cross sections of each final states at LHeC and ep collider achieve maximum values at the different PDF. Biggest uncertainty of PDFs is found in $c\bar{c}$ final state at $\sqrt{s} = 3.74 \text{ TeV}$.

ACKNOWLEDGMENTS

The authors would like to thank S. Sultansoy and G. Unel for useful discussion.

-
- [1] U. Kaya, S. Sultansoy, G. Unel, arXiv:hep-ph/1211.5061v1.
[2] J.L. Abelleira Fernandez, C. Adolphsen, A. N. Akay et al. [LHeC Study Group], J. Phys. G: Nucl. Part. Phys. 39 (2012) 075001.

- [3] Z. Sullivan and P.M. Nadolsky, in Proceedings of the APS/ DPF/DPB Summer Study on the Future of Particle Physics (2001), edited by R. Davidson and C. Quigg, hep-ph/0111358.
- [4] E. Boos et al. (CompHEP Collaboration), Nucl. Instrum. Methods Phys. Res., Sect. A 534, 250 (2004).
- [5] ATLAS Detector and Physics Performance Technical Design Report. CERN/LHCC/99-14/15, (1999).
- [6] M. S. Chanowitz et al., Nucl. Phys. B 153, 402 (1979).
- [7] J. Pumplin et al., JHEP 0207 (2002) 012.
- [8] C.Targett-Adams, arXiv:hep-ex/0507024v1, (2005).
- [9] C.W Bauer and M. Neubert. available at: <http://pdg.lbl.gov/2012/reviews/rpp2012-rev-heavy-quark-eff-th.pdf> (2011)
- [10] S. Sultansoy, Eur. Phys. J 33, 1064–1066 (2004) .
- [11] A. N. Akay, H. Karadeniz and S. Sultansoy. Int. J. Mod. Phys. A 25, 4589 (2010)
- [12] F. Zimmermann et al. SLAC-PUB-15102, (2011)
- [13] J. B. Dainton et al. arXiv:hep-ex/0603016v2. (2006)
- [14] E. Arikani, H. Aksakal, Nucl. Instrum. Methods Phys. Res., Sect. A 683 (2012) 63-70.
- [15] H. Aksakal et al., Proceedings of PAC (2005), p. 1207.
- [16] H. Aksakal et al., Nucl. Instrum. Methods Phys. Res., Sect. A Vol. 567, Issue 2-3, p287 (2007).
- [17] K. Yokoya, CAIN223, the code available at: <http://www-acc-theory.kek.jp/members/cain/default.html>.
- [18] W.-M. Yao et al., (Particle Data Group) Journal of Physics G 33, 1 (2006).
- [19] B. Holdom, JHEP 0608, 076 (2006); B. Holdom, JHEP 0703, 063 (2007).
- [20] B. Holdom, JHEP08, 069 (2007).

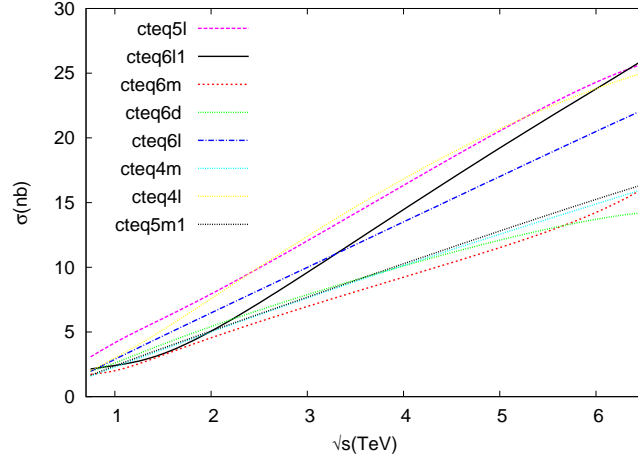


Figure 2. Total cross section versus center of mass energy values (\sqrt{s}) for different PDF distribution

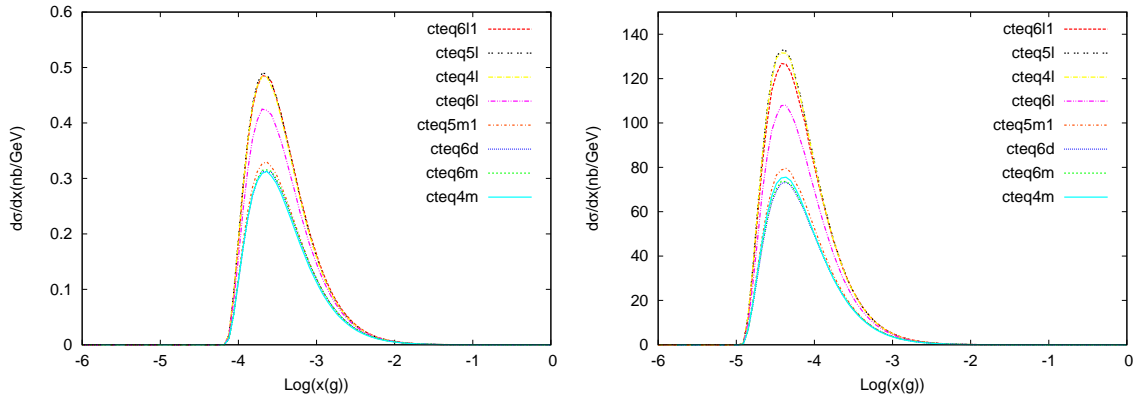


Figure 3. Differential cross section versus the $x(g)$ in $b\bar{b}$ (left) and $c\bar{c}$ (right) for LHeC Type-1

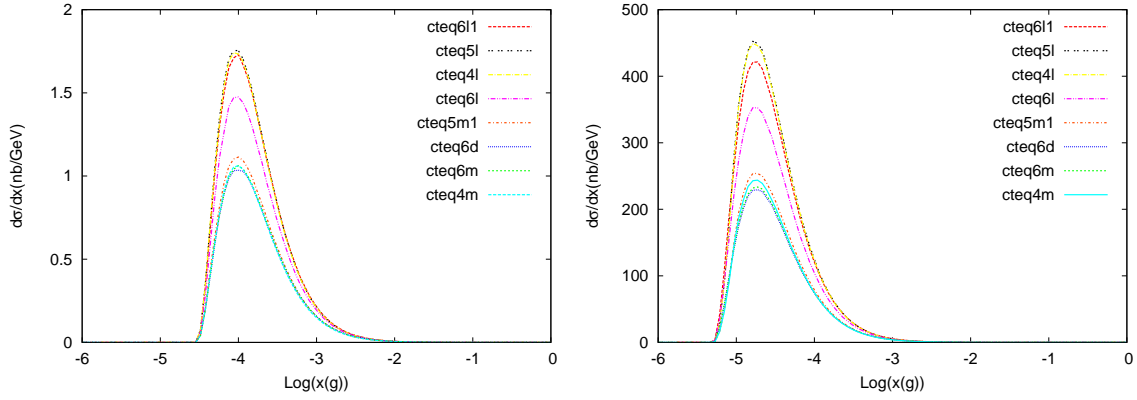


Figure 4. Differential cross section versus the $x(g)$ in $b\bar{b}$ (left) and $c\bar{c}$ (right) for LHeC Type-2

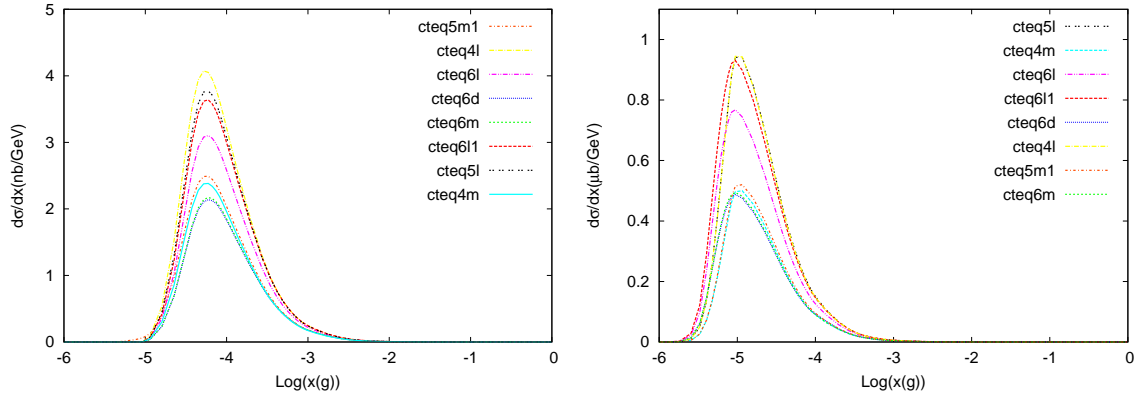


Figure 5. Differential cross section versus the $x(g)$ in $b\bar{b}$ (left) and $c\bar{c}$ (right) for ep collider-1

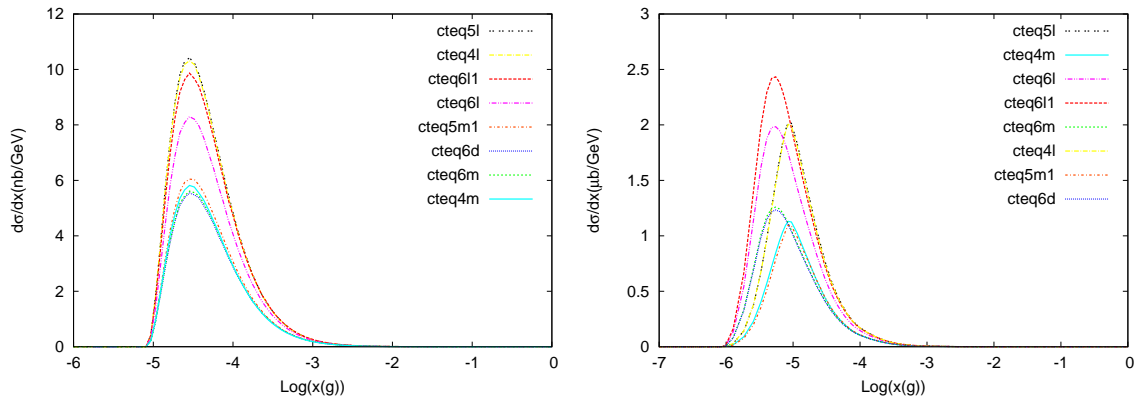


Figure 6. Differential cross section versus the $x(g)$ in $b\bar{b}$ (left) and $c\bar{c}$ (right) for ep collider-2